HHS Public Access

Author manuscript

Acc Chem Res. Author manuscript; available in PMC 2016 February 02.

Published in final edited form as:

Acc Chem Res. 2015 August 18; 48(8): 2280–2287. doi:10.1021/acs.accounts.5b00227.

New Ru(II) Complexes for Dual Photoreactivity: Ligand Exchange and $^1O_2$ Generation

Jessica D. Knoll, **Bryan A. Albani**, and **Claudia Turro***

Department of Chemistry and Biochemistry, The Ohio State University, Columbus, Ohio 43210, United States

CONSPECTUS

Uncovering the factors that govern the electronic structure of Ru(II)–polypyridyl complexes is critical in designing new compounds for desired photochemical reactions, and strategies to tune excited states for ligand dissociation and $^1O_2$ production are discussed herein. The generally accepted mechanism for photoinduced ligand dissociation proposes that population of the dissociative triplet ligand field (^{3}LF) state proceeds through thermal population from the vibrationally cooled triplet metal-to-ligand charge transfer (^{3}MLCT) state; however, temperature-dependent emission spectroscopy provides varied activation energies using the emission and ligand exchange quantum yields for $[Ru(bpy)_2(L)_2]^{2+}$ (bpy = 2,2′-bipyridine; L = CH_3CN or py). This suggests that population of the ^{3}LF state proceeds from the vibrationally excited ^{3}MLCT state. Because the quantum yield of ligand dissociation for nitriles is much more efficient than that for py, steric bulk was introduced into the ligand set to distort the pseudo-octahedral geometry and lower the energy of the ^{3}LF state. The py dissociation quantum yield with 500 nm irradiation in a series of $[Ru(tpy)(NN)(py)]^{2+}$ complexes (tpy = 2,2′:6′,2″-terpyridine; NN = bpy, 6,6′-dimethyl-2,2′-bipyridine (Me_2bpy), 2,2′-biquinoline (biq)) increases by 2–3 orders of magnitude with the sterically bulky Me_2bpy and biq ligands relative to bpy. Ultrafast transient absorption spectroscopy reveals population of the ^{3}LF state within 3–7 ps when NN is bulky, and density functional theory calculations support stabilized ^{3}LF states. Dual activity via ligand dissociation and $^1O_2$ production can be achieved by careful selection of the ligand set to tune the excited-state dynamics. Incorporation of an extended π system in Ru(II) complexes such as $[Ru(bpy)(dppn)(CH_3CN)_2]^{2+}$ (dppn = benzo[*i*]dipyrido[3,2-*a*:2′,3′-*c*]phenazine) and $[Ru(tpy)(Me_2dppn)(py)]^{2+}$ (Me_2dppn = 3,6-dimethylbenzo[*i*]dipyrido[3,2-*a*:2′,3′-*c*]phenazine) introduces low-lying, long-lived dppn/Me_2dppn $^3\pi\pi^*$ excited states that generate $^1O_2$. Similar to $[Ru(bpy)_2(CH_3CN)_2]^{2+}$, photodissociation of CH_3CN occurs upon irradiation of $[Ru(bpy)(dppn)(CH_3CN)_2]^{2+}$, although with lower efficiency because of the presence of the $^3\pi\pi^*$ state. The steric bulk in $[Ru(tpy)(Me_2dppn)(py)]^{2+}$ is critical in facilitating the photoinduced py dissociation, as the analogous complex $[Ru(tpy)(dppn)(py)]^{2+}$ produces $^1O_2$ with near-unit efficiency. The ability to tune the relative energies of the excited states provides a means to design potentially more active drugs for photochemotherapy because the photorelease of drugs can be coupled to the therapeutic action of reactive oxygen species, effecting cell death via two different mechanisms. The lessons learned

*Corresponding Author: turro.1@osu.edu.

Notes

The authors declare no competing financial interest.

about tuning of the excited-state properties can be applied to the use of Ru(II)–polypyridyl compounds in a variety of applications, such as solar energy conversion, sensors and switches, and molecular machines.

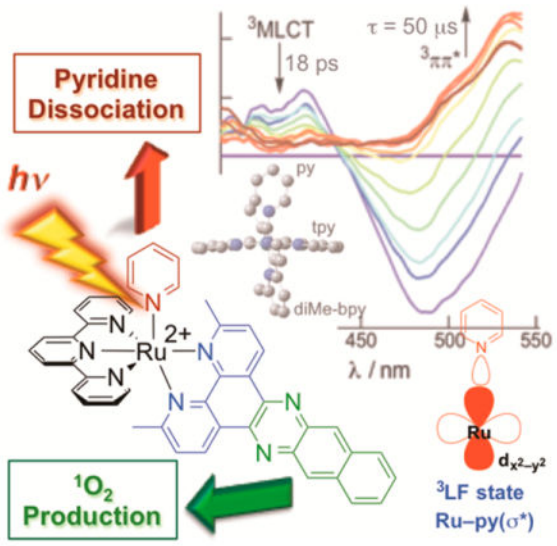

INTRODUCTION

Excited states of Ru(II) complexes have been used in solar energy conversion,[1–5] in charge transfer reactions,[6,7] as sensors and switches,[8,9] and as potential therapeutic agents in photochemotherapy (PCT) and imaging.[10–16] Although many complexes are derived from $[Ru(bpy)_3]^{2+}$ (bpy = 2,2′-bipyridine) (Figure 1a),[17] these applications often have different demands. For example, the excited-state redox potential is crucial in solar energy schemes and charge transfer reactions, which often require long-lived triplet metal-to-ligand charge transfer (^{3}MLCT) excited states, whereas strong luminescence and sensitivity to the environment have been important in sensor applications. In contrast, complexes developed for PCT typically require high yields of photo-induced ligand exchange for prodrug delivery or to achieve binding of the metal to biomolecules, which in turn results in short ^{3}MLCT lifetimes with low luminescence yields. In order to tune the relative energies of the excited states to achieve the desired properties, an understanding of the factors that affect the electronic structure of Ru(II) complexes is necessary.

The electronic structure and excited-state dynamics of $[Ru(bpy)_3]^{2+}$ and related complexes have been the subject of numerous reviews.[17] Figure 1b presents a simplified diagram showing the frontier molecular orbitals (MOs) of $[Ru(bpy)_3]^{2+}$ in a pseudo-octahedral field, for which the lowest-energy ^{1}MLCT transition has a maximum at 452 nm (ε = 14 600 M^{-1} cm^{-1}) and the bpy $\pi\pi^*$ transitions are observed at 285 nm (ε = 87 000 M^{-1} cm^{-1}) in water.[17] Ultrafast ^{1}MLCT → ^{3}MLCT intersystem crossing (ISC) was reported in $[Ru(bpy)_3]^{2+}$ (15–40 fs),[18,19] and to our knowledge, significantly lower ISC rates have not been reported for Ru(II) complexes. Therefore, with the exception of charge injection into semiconductors,[20] the excited-state chemistry of Ru(II) complexes takes place from the

triplet manifold. The low-lying triplet excited states of $[Ru(bpy)_3]^{2+}$ are schematically shown in Figure 1c, where the metal-centered triplet ligand field (^{3}LF) state(s) involve transitions from the t_{2g}-type orbitals to the e_g-type orbitals, and the triplet ligand-centered (^{3}LC) states arise from movement of an electron from the bpy(π) MOs to the bpy(π^*) MOs. In $[Ru(bpy)_3]^{2+}$, the ^{3}MLCT state is emissive (λ_{em} = 607 nm, τ = 620 ns, Φ = 0.042 in water at 298 K).[17] The lifetimes of Ru(II) complexes in which the ^{3}LC excited state falls below the ^{3}MLCT state are similar to those of the $^3\pi\pi^*$ state of the free ligand, and these complexes generally are not emissive, exhibit long lifetimes, and feature efficient $^1O_2$ sensitization.[21–24] In contrast, stabilization of the ^{3}LF states results in photoinduced ligand exchange, which may be accomplished by introducing distortions around the metal center. These distortions reduce the orbital overlap and lower the energy of the e_g-type orbitals,[15] thus decreasing the energy of the ^{3}LF states, sometimes below that of the ^{3}MLCT state.[25]

The present Account focuses on the effect of structural changes to ruthenium(II) complexes on the excited-state properties and reactivity. Of particular interest are compounds that undergo photoinduced ligand exchange and those that generate $^1O_2$, as well as new complexes designed in such a way that both processes are operative in the same complex upon irradiation with low-energy light. This dual reactivity has the potential to be useful in applications related to PCT, where cell death may be achieved via two different mechanisms by the same molecule.

ACTIVATION BARRIER TO PHOTOINDUCED LIGAND EXCHANGE

It is well-established that deactivation of the emissive ^{3}MLCT state in Ru(II) complexes proceeds via thermal population of the ^{3}LF states, which reduces the lifetime of the former. For applications that require charge transfer or high luminescence quantum yields, researchers aim to maximize the gap between the ^{3}MLCT and ^{3}LF states, which minimizes deactivation through the latter. In contrast, maximizing photoinduced ligand exchange of ruthenium(II) complexes, such as in the release of active molecules to biological targets and to gain understanding of their function, to inhibit enzymes, and to generate reactive species that can covalently bind to DNA, requires efficient population of the dissociative ^{3}LF states.[11,13–15] One limitation is the relatively low quantum yield of ligand exchange in some complexes.

It has been generally accepted that the formation of photosubstituted products in Ru(II)–polypyridyl complexes proceeds through thermal population of the dissociative ^{3}LF state(s) from the vibrationally cooled emissive ^{3}MLCT state ($^3MLCT_{v=0}$).[26] It is also established that deactivation of the emissive $^3MLCT_{v=0}$ state proceeds via population of the low-lying ^{3}LF state(s), as depicted in Figure 2a. If it is assumed that the only source of photoinduced ligand exchange is population of the ^{3}LF state from $^3MLCT_{v=0}$, then Arrhenius plots of both the photochemical yield and the emission intensity should give rise to the same activation energy, E_a (Figure 2a).

Plots of ln(Φ) versus 1/T for the photoanation reactions of $[Ru(bpy)_2(L)_2]^{2+}$ (L = py, CH_3CN) to generate the corresponding $[Ru(bpy)_2(L)Cl]^+$ product in the presence of excess tetrabutylammonium chloride (TBACl) in CH_2Cl_2 were reported to result in $E_a \approx 700$

cm^{-1},[27] whereas changes in the emission lifetime of $[Ru(bpy)_2(py)_2]^{2+}$ with temperature result in E_a = 2758 cm^{-1}.[28] However, these activation barriers were measured in two different temperature regimes, which can account for the different values. In addition, there have been other reports on the discrepancy between the magnitudes of E_a determined from emission and photochemical yields as well as from emission intensity and lifetime data.[28,29] The concluding remarks in both reports point to possible direct population of the ^{3}LF state from the ^{1}MLCT state together with population of the emissive ^{3}MLCT state.[28,29]

To gain further understanding of the photoinduced ligand exchange in $[Ru(bpy)_2(L)_2]^{2+}$ (L = CH_3CN, py), the activation energies for photoanation to generate the corresponding complexes $[Ru(bpy)_2(L)Cl]^+$, E_a^P, were measured over the same temperature range as for the value from the changes in emission intensity, E_a^{Em}, in 4:1 ethanol/methanol above the glass transition temperature.[30] The experiments were conducted in a cryostat placed in the sample compartment of the fluorimeter, and the decrease in the emission intensity as the temperature was raised was monitored in the absence of anion immediately after excitation to determine E_a^{Em}. The change in emission intensity as a function of irradiation time in the presence of 20 mM TBACl was used to calculate the value of E_a^P, and the results are listed in Table 1.[30] It is evident from Table 1 that for both complexes the value of E_a^P is significantly lower than that of E_a^{Em}. It may be concluded that the ligand exchange does not proceed from $^3MLCT_{v=0}$, as shown in Figure 2a. Instead, the population of the dissociative ^{3}LF state must have a different origin, as previously proposed by us,[31] and may include direct ISC from the Franck–Condon ^{1}MLCT state, internal conversion (IC) from a higher-energy ^{3}MLCT state, or IC from the vibrationally excited lowest-energy ^{3}MLCT state ($^3MLCT_{v\gg1}$). The latter situation is depicted in Figure 2b, where vibrational cooling competes with IC from a vibrational level well above v = 0, as previously proposed from ultrafast work.[32]

In order for efficient ligand dissociation to be observed, population of the ^{3}LF state must compete with generation of $^3MLCT_{v=0}$. In systems such as $[Ru(bpy)_2(CH_3CN)_2]^{2+}$, there must be strong vibrational coupling between the MLCT (singlet or triplet) and ^{3}LF states, which is reduced in $[Ru(bpy)_2(py)_2]^{2+}$. For example, strong vibrational coupling is believed to play a role in the ultrafast ISC of <100 fs in $Cr(acac)_3$ (acac = acetylacetonate), but interestingly, it decreases by over an order of magnitude when the ligand's peripheral methyl groups are replaced by *tert*-butyl substituents in Cr(*t*-Bu-acac)$_3$.[33] In addition to nitriles, thioethers undergo photoinduced ligand dissociation with greater quantum yields than their ammine counterparts, and the ^{3}MLCT states of the former were calculated to exhibit elongated Ru–S bonds, which may be related to MLCT/LF mixing.[34]

ENHANCED PHOTOINDUCED LIGAND EXCHANGE WITH STERIC BULK

To increase the quantum yield for pyridine exchange through enhanced population of the ^{3}LF state, sterically bulky ligands were incorporated to distort the pseudo-octahedral geometry around the metal center. The decrease in the energy of the ^{3}LF state(s) as a function of increasing steric bulk was demonstrated for a series of complexes $[Ru(NN)_3]^{2+}$ with NN = bpy, 6-methyl-2,2′-bipyridine (6-Mebpy), and 4,4′,6,6′-tetramethyl-2,2′-

bipyridine (Me_4bpy) using ultrafast transient absorption (TA) spectroscopy.[25] On the basis of the difference in the decay of the ^{3}MLCT state and recovery of the ground state, it was shown that the rate of population of a ^{3}LF state from the ^{3}MLCT state increased by an order of magnitude in going from $[Ru(6\text{-}Mebpy)_3]^{2+}$ to the more sterically demanding $[Ru(Me_4bpy)_3]^{2+}$, with ^{3}MLCT lifetimes of 1.6 and 0.16 ps, respectively.[25] Distortions around the metal lead to a decrease in the calculated energy of the ^{3}LF state by ~4000 cm^{-1} in $[Ru(6\text{-}Mebpy)_3]^{2+}$ and ~7000 cm^{-1} in $[Ru(Me_4bpy)_3]^{2+}$ relative to that in $[Ru(bpy)_3]^{2+}$. Therefore, while the ^{3}LF state lies above the ^{3}MLCT state in the latter, it falls below the ^{3}MLCT state in the former, resulting in fast ^{3}MLCT decay to populate the ^{3}LF state.

The enhanced population of the ^{3}LF state(s) in ruthenium-(II) complexes with bulky ligands leads to greater photo-induced ligand exchange. For example, photodissociation of 2,2′-biquinoline (biq) from $[Ru(biq)(phen)_2]^{2+}$ (phen = 1,10-phenathroline) and $[Ru(biq)_2(phen)]^{2+}$ in H_2O occurs with λ_{irr} ≥600 nm, while this photoactivity is not observed in $[Ru(phen)_3]^{2+}$.[35] The crystal structures of the biq complexes reveal lengthened Ru–N bonds compared with those in $[Ru(phen)_3]^{2+}$ as well as significant twisting of biq along the C–C bond connecting the two quinoline moieties and bending of biq by ~20° out of the normal plane. Similar photoreactivity was reported for $[Ru(biq)_2(bpy)]^{2+}$ in CH_3CN.[36] The presence of methyl, phenyl, or chloro substituents positioned toward the Ru(II) center also induces geometric distortions and facilitates photosubstitution of the bulky bidentate ligands with solvent molecules.[15,37,38]

To increase the photodissociation quantum yield of pyridine from pseudo-octahedral ruthenium(II) complexes, steric bulk was introduced in the series $[Ru(tpy)(NN)(py)]^{2+}$ (tpy = 2,2′:6′,2″-terpyridine; NN = bpy, 6,6′-dimethyl-2,2′-bipyridinep(Me_2bpy), biq) (Figure 3).[39] The lowest-energy electronic transition observed in $[Ru(tpy)(NN)(py)]^{2+}$ (NN = bpy, Me_2bpy) is the Ru(dπ) → tpy(π^*) ^{1}MLCT transition with maxima at 468 nm (8120 M^{-1} cm^{-1}) and 471 nm (8020 M^{-1} cm^{-1}), respectively, whereas that in $[Ru(tpy)(biq)(py)]^{2+}$ is assigned as the Ru(dπ) → biq(π^*) ^{1}MLCT transition at 530 nm (9020 M^{-1} cm^{-1}). Photoinduced exchange of py is not observed in $[Ru(tpy)(bpy)(py)]^{2+}$ (Φ_{500} < 0.0001), but irradiation of $[Ru(tpy)(Me_2bpy)(py)]^{2+}$ and $[Ru(tpy)(biq)\text{-}(py)]^{2+}$ in CH_3CN generates the corresponding products $[Ru(tpy)(NN)(CH_3CN)]^{2+}$ (NN = Me_2bpy, biq) with Φ_{500} = 0.16(1) and 0.033(1), respectively (Table 2). All three complexes are stable in CH_3CN and H_2O solutions in the dark for at least 24 h at room temperature.

The crystal structures reveal key structural distortions in $[Ru(tpy)(Me_2bpy)(py)]^{2+}$ and $[Ru(tpy)(biq)(py)]^{2+}$ afforded by steric bulk from the bidentate ligands compared with $[Ru(tpy)(bpy)(py)]^{2+}$. In particular, the angle between the plane defined by the bidentate ligand and that of the tpy ligand, determined to be 83.34° in $[Ru(tpy)(bpy)(py)]^{2+}$, is reduced to 67.87° and 61.89° in $[Ru(tpy)(Me_2bpy)(py)]^{2+}$ and $[Ru(tpy)(biq)(py)]^{2+}$, respectively, similar to distortions reported for related complexes.[35,40,41] More importantly, the pyridine ligand in the Me_2bpy and biq complexes is distorted relative to that in $[Ru(tpy)(bpy)(py)]^{2+}$. The enhanced photoinduced ligand exchange efficiency is correlated to structural distortions, which are believed to stabilize ^{3}LF states and weaken the Ru–py σ bond.

Ultrafast TA spectroscopy reveals the consequences of added steric bulk on the excited-state dynamics of $[Ru(tpy)(Me_2bpy)\text{-}(py)]^{2+}$ compared with $[Ru(tpy)(bpy)(py)]^{2+}$ (Figure 4). For both complexes, the spectra feature a ground-state bleach centered at ~470 nm as well as positive transient absorption signals at ~375 and >500 nm associated with the $Ru(d\pi) \rightarrow tpy(\pi^*)$ ^{3}MLCT state.[42] While the spectral features are similar for the two complexes, stark differences are observed in the kinetics. The absorption changes of the bleach signal at 470 nm for $[Ru(tpy)(bpy)(py)]^{2+}$ in CH_3CN (Figure 4a) can be fitted to a biexponential decay with τ_1 = 28 ps (8%) and τ_2 = 544 ps (92%). The absorption changes associated with the reduced ligands in the ^{3}MLCT states in the 350–420 nm range display a broad maximum at ~370 nm at 1–10 ps delay but sharpen and red-shift to ~375 nm with a shoulder at ~390 nm at later times. These changes are accompanied by biexponential decays at 375 and 575 nm with $\tau_1 \approx 3$ ps and a long component with $\tau_2 \approx 500$ ps. The Ru → bpy ^{1}MLCT state is preferentially excited at 350 nm, resulting in fast ISC to the corresponding Ru → bpy ^{3}MLCT state with maximum at ~370 nm associated with reduced bpy. This state decays to populate the Ru → tpy ^{3}MLCT state within ~23 ps, with a maximum at ~375 nm and a shoulder at ~410 nm, similar to the spectral features for $[Ru(tpy)_2]^{2+}$.[43,44] Since the 28 ps component represents a minor fraction (8%) of the bleach recovery, it corresponds to changes in absorption during ^{3}MLCT(bpy) → ^{3}MLCT(tpy) IC. The 23 ps component for the ^{3}MLCT(bpy) → ^{3}MLCT-(tpy) IC is consistent with the value of 26 ps previously reported for a related complex with two low-lying ^{3}MLCT states.[45]

Excitation of the red edge of the Ru → tpy ^{1}MLCT absorption band of $[Ru(tpy)(bpy)(py)]^{2+}$ with λ_{exc} = 568 nm produces a bleach signal that can be fitted to τ_1 = 6 ps (12%) and τ_2 = 437 ps (88%); similar kinetics are observed at 375 nm. The 6 ps component is attributed to vibrational relaxation in the Ru → tpy ^{3}MLCT state, which then decays to regenerate the ground state with τ = 470 ps (Figure 5a). As expected, the 23–28 ps component is not present with 568 nm excitation. The 470 ps lifetime of the Ru → tpy ^{3}MLCT state compares well to those of $[Ru(tpy)_2]^{2+}$ (120 ps in CH_3CN and 250 ps in H_2O).[42–44]

The TA spectra that result from 568 nm excitation of $[Ru(tpy)(Me_2bpy)(py)]^{2+}$ are shown in Figure 4b, where selective population of the Ru → tpy ^{1}MLCT state results in observation of the Ru → tpy ^{3}MLCT absorption signals at ~375 and ~400 nm with monoexponential decay of τ = 6 ps and a biexponential bleach recovery at 470 nm with τ_1 = 7 ps (16%) and τ_2 = 38 ps (84%). The 6–7 ps component can be ascribed to IC from the Ru → tpy ^{3}MLCT state to populate the ^{3}LF state, which competes with vibrational cooling in the former, and the ^{3}LF state regenerates the ground state with time constant of 38 ps (Figure 5b). Excitation of $[Ru(tpy)\text{-}(Me_2bpy)(py)]^{2+}$ at 350 nm provides similar kinetics but with an additional ~3 ps component associated with decay of the Ru → Me_2bpy ^{3}MLCT state (Figure 5b). These experiments are consistent with generation of the ^{3}LF state within 3–7 ps, which then deactivates via ligand dissociation and thermal decay to the ground state. It is evident in the ultrafast TA data for $[Ru(tpy)(Me_2bpy)(py)]^{2+}$ in Figure 4b that the ground state does not fully recover in the final trace (2 ns), consistent with formation of the monosubstituted CH_3CN photoproduct, $[Ru(tpy)(Me_2bpy)(CH_3CN)]^{2+}$. However, the kinetics of the photoproduct formation cannot be determined because of its spectral overlap with the

ground and excited states of the starting compound and the relatively small quantity of photoproduct formed.

Distortions around the metal center in $[Ru(tpy)(Me_2bpy)\text{-}(py)]^{2+}$ compared with $[Ru(tpy)(bpy)(py)]^{2+}$ can explain the differences in excited-state dynamics, resulting in a lower-energy ^{3}LF state in the former that falls below the Ru → tpy ^{3}MLCT state (Figure 5). The lower-energy ^{3}LF state leads to enhanced ligand exchange for the Me_2bpy complex; the ^{3}LF lifetime of $[Ru(tpy)(Me_2bpy)(py)]^{2+}$ is similar to those of Ru(II) complexes with sterically bulky ligands, 45 ps for $[Ru(6\text{-}Mebpy)_3]^{2+}$ and 7.5 ps for $[Ru(Me_4bpy)_3]^{2+}$.[25] The formation of a pentacoordinate intermediate (PCI) from the ^{3}LF state is possible, such that the dynamics of the ground-state regeneration are due to geminate recombination of the PCI and pyridine. However, the cage escape and geminate recombination kinetics for the related complex $[Ru\text{-}(bpy)_2(NA)_2]^{2+}$ (NA = nicotinamide) in water were reported as 377 and 263 ps, respectively.[32] This order of magnitude difference between the bleach recovery of $[Ru(tpy)(Me_2bpy)\text{-}(py)]^{2+}$ and $[Ru(bpy)_2(NA)_2]^{2+}$ is inconsistent with the 38 ps component assigned as geminate recombination. Ultrafast population of the ^{3}LF state from the Ru → tpy ^{1}MLCT or vibrationally excited ^{3}MLCT state, $^3MLCT_{\nu\Delta1}$, to afford py dissociation is supported by efficient ligand exchange for $[Ru(tpy)(Me_2bpy)(py)]^{2+}$ with low-energy light (λ_{irr} ≥600 nm) and the excited-state dynamics measured with 568 nm excitation. This finding is also consistent with the differences in E_a^{Em} and E_a^{P} measured for $[Ru(bpy)_2(py)_2]^{2+}$ (Table 1).

Density functional theory (DFT) calculations on $[Ru(tpy)\text{-}(NN)(py)]^{2+}$ (NN = bpy, Me_2bpy) show that the unoccupied $d_{x^2-y^2}$ orbital, directed along the Ru–py bond, is at a lower energy than the d_{z^2} orbital in each complex. Therefore, population of the lowest-energy LF state results in additional electron density in the d_{x^2-2} orbital, weakening the Ru–py bond. The distortions in $[Ru(tpy)(Me_2bpy)(py)]^{2+}$ lower the calculated d_{x^2-2} orbital energy by 0.82 eV relative to $[Ru(tpy)(bpy)(py)]^{2+}$, consistent with stabilization of the LF states with Ru–py(σ^*) character.

DUAL ACTIVITY: PHOTOINDUCED LIGAND EXCHANGE AND $^1O_2$ GENERATION

$[Ru(bpy)(dppn)(CH_3CN)_2]^{2+}$ (dppn = benzo[*i*]dipyrido[3,2-*a*:2′,3′-*c*]phenazine) (Figure 6) combines the ligand exchange photochemistry of $[Ru(bpy)_2(CH_3CN)_2]^{2+}$ and the $^1O_2$ production of $[Ru(bpy)_2(dppn)]^{2+}$ to enhance cellular photo-toxicity.[46] The electronic absorption spectrum of $[Ru(bpy)\text{-}(dppn)(CH_3CN)_2]^{2+}$ features a ^{1}MLCT maximum at 430 nm (11 000 M^{-1} cm^{-1}) and dppn-centered $^1\pi\pi^*$ transitions at 382 nm (11 100 M^{-1} cm^{-1}) and 405 nm (13 500 M^{-1} cm^{-1}). The lowest-energy excited state of the complex is the dppn-centered $^3\pi\pi^*$ state with $\tau = 20$ μs in CH_3CN, similar to those of $[Ru(bpy)_2(dppn)]^{2+}$ ($\tau = 33$ μs in CH_3CN) and free dppn ($\tau = 18$ μs in $CHCl_3$).[21] In $[Ru(bpy)_2(CH_3CN)_2]^{2+}$, both the lowest-energy ^{3}MLCT excited state ($\tau = 51$ ps) and the low-lying ^{3}LF state are populated upon ultrafast excitation, and the complex undergoes efficient photoinduced ligand exchange.[31]

Irradiation of $[Ru(bpy)(dppn)(CH_3CN)_2]^{2+}$ in water promotes sequential substitution of the two CH_3CN ligands (λ_{irr} = 400 nm); the first step forms $[Ru(bpy)(dppn)\text{-}(CH_3CN)(OH_2)]^{2+}$ with Φ_{400} = 0.002(3), which is 2 orders of magnitude lower than that in $[Ru(bpy)_2(CH_3CN)_2]^{2+}$ (Φ_{400} = 0.21).[31] The quantum yield for production of $^1O_2$ (Φ_Δ) from the $^3\pi\pi^*$ state of $[Ru(bpy)(dppn)(CH_3CN)_2]^{2+}$ is 0.72(2), which is slightly lower than that of $[Ru(bpy)_2(dppn)]^{2+}$ (0.88(2)). The lower yields of ligand exchange and $^1O_2$ generation in $[Ru(bpy)(dppn)(CH_3CN)_2]^{2+}$ relative to the parent complexes are explained by competitive population of the ^{3}LF and $^3\pi\pi^*$ states. A phthalocyanine Ru(II) complex with bound NO ligands was previously shown to produce $^1O_2$ with Φ_Δ = 0.29 and photorelease NO.[47]

Ultrafast TA spectroscopy reveals the excited-state dynamics of $[Ru(bpy)(dppn)(CH_3CN)_2]^{2+}$. Because of spectral overlap of the ^{1}MLCT and $^1\pi\pi^*$ bands, one cannot be accessed selectively. Excitation in the 300 to 400 nm range results in the observation of both the ^{3}MLCT and $^3\pi\pi^*$ states within the laser pulse, with absorption at ~360 and ~540 nm, respectively (Figure 7). Additionally, the lower-lying $^3\pi\pi^*$ state is also populated from the ^{3}MLCT state through IC with τ = 22 ps (Figure 7). Although the observed ligand exchange is expected to occur through the ^{3}LF state, the latter was not detected, likely because of its low quantum yield and weak oscillator strength.

$[Ru(tpy)(Me_2dppn)(py)]^{2+}$ (Me_2dppn = 3,6-dimethylbenzo-[*i*]dipyrido[3,2-*a*:2′,3′-*c*]phenazine) (Figure 8) undergoes both pyridine dissociation and $^1O_2$ production with visible light. The Me_2dppn ligand causes geometric strain similar to that caused by Me_2bpy, but the complex maintains the Me_2dppn $^3\pi\pi^*$ lowest-energy excited state.[48] $[Ru(tpy)(Me_2dppn)(py)]^{2+}$ absorbs strongly in the visible region with dppn-centered $^1\pi\pi^*$ transitions at 382 nm (11 400 M^{-1} cm^{-1}) and 404 nm (12 400 M^{-1} cm^{-1}) and a ^{1}MLCT peak at 486 nm (12 900 M^{-1} cm^{-1}). When photolyzed in CH_3CN (λ_{irr} = 500 nm), $[Ru(tpy)(Me_2dppn)(CH_3CN)]^{2+}$ is formed with Φ_{500} = 0.053(1) in the absence of O_2, but ligand exchange is not observed in $[Ru(tpy)(dppn)(py)]^{2+}$ ($\Phi_{500} < 10^{-4}$), which lacks steric strain (Table 2). Photosensitization of $^1O_2$ by $[Ru(tpy)\text{-}(Me_2dppn)(py)]^{2+}$ occurs with Φ_Δ = 0.69(9), which is lower than the value of 0.98(6) measured for $[Ru(tpy)(dppn)(py)]^{2+}$ (λ_{irr} = 460 nm), as listed in Table 2. The reduced quantum yield for $[Ru(tpy)(Me_2dppn)(py)]^{2+}$ can be attributed to competitive deactivation through the ^{3}LF state afforded by distortions around the metal. Competitive population of excited states also explains the lower ligand exchange quantum yield of $[Ru(tpy)(Me_2dppn)(py)]^{2+}$ relative to $[Ru(tpy)(Me_2bpy)\text{-}(py)]^{2+}$.

Following selective Ru → tpy ^{1}MLCT excitation of $[Ru(tpy)(dppn)(py)]^{2+}$ and $[Ru(tpy)(Me_2dppn)(py)]^{2+}$ at 568 nm, the Ru → tpy ^{3}MLCT state of $[Ru(tpy)(Me_2dppn)\text{-}(py)]^{2+}$ is observed at ~390 and ~415 nm within the laser pulse, along with a strong ground-state bleach centered at ~480 nm (Figure 9a). Although the signal at 535 nm corresponding to the Me_2dppn $^3\pi\pi^*$ state is not observed at early times, it evolves with τ_1 = 2 ps (28%) and τ_2 = 17 ps (72%), concomitant with the decay of the ^{3}MLCT signals fitted to τ_1 = 3 ps (13%) and τ_2 = 18 ps (87%) at 415 nm and changes in the bleach signal with τ_1 = 1 ps (16%) and τ_2 = 18 ps (84%). The ~2 ps decay is believed to have contributions from ISC, IC, and vibrational cooling, while the 18 ps component is assigned to population of the $^3\pi\pi^*$ state from the ^{3}MLCT state. Similar spectral features and kinetics were measured for $[Ru(tpy)\text{-}(dppn)(py)]^{2+}$ in CH_3CN under 568 nm excitation, for which the growth of the 540 nm peak

and bleach recovery at 470 nm can be fitted to τ_1 = 1 ps (21%) and τ_2 = 22 ps (79%). The long component is ascribed to IC from the ^{3}MLCT state to the dppn $^3\pi\pi^*$ state, while the short component is related to ISC, IC, and vibrational cooling processes.

The Jablonski diagram of [Ru(tpy)(Me$_2$dppn)(py)]$^{2+}$, depicted in Figure 9b, shows that IC from the Ru → tpy ^{3}MLCT state to the dppn $^3\pi\pi^*$ state occurs with τ = 18 ps in the Me$_2$dppn complex, as opposed to 22 ps in [Ru(tpy)-(dppn)(py)]$^{2+}$. Since photoinduced ligand exchange is observed in [Ru(tpy)(Me$_2$dppn)(py)]$^{2+}$ with λ_{irr} ≥550 nm, low-energy light must populate the dissociative ^{3}LF state. The similarity in the $^3\pi\pi^*$ lifetimes of [Ru(tpy)(dppn)(py)]$^{2+}$ and [Ru(tpy)(Me$_2$dppn)(py)]$^{2+}$ (τ = 50 and 47 μs, respectively; λ_{exc} = 355 nm, fwhm ≈ 8 ns) is consistent with the ^{3}LF state being located at a higher energy, as shown in Figure 9b.

CONCLUSIONS

The ability of Ru(II) complexes to undergo both photoinduced ligand exchange and $^1O_2$ generation efficiently provides a means to design potentially more active PCT therapeutics. In particular, photorelease of drugs can be coupled to the activity of reactive oxygen species, enabling these compounds to effect cell death via two different mechanisms upon visible-light irradiation. Steric strain can be used to lower the energy of the metal-centered state(s), resulting in greater yields of ligand photodissociation, even when these states(s) are not the lowest in energy. Mixing between the ^{3}LF state(s) and MLCT and/or LC states is believed to play an important role in efficient photoinduced ligand exchange, which is greater when these states are closer in energy. Work is underway to gain further understanding of the coupling between states with the goal of increasing the ligand exchange yields in these dual-action complexes while retaining relatively high sensitization of $^1O_2$ upon irradiation in the photodynamic window (600–900 nm).

Acknowledgments

The authors thank the National Science Foundation (CHE-1465067) and the National Institutes of Health (R01 EB16072) for partial support and the resources of the Center for Chemical and Biophysical Dynamics (CCBD) at OSU.

References

1. Serpone N, Pelizzetti E, Gratzel M. Photosensitization of Semiconductors with Transition Metal Complexes – A Route to the Photoassisted Cleavage of Water. Coord Chem Rev. 1985; 64:225–245.
2. Thompson DW, Ito A, Meyer TJ. [Ru(bpy)$_3$]$^{2+}$* and Other Remarkable Metal-to-Ligand Charge Transfer (MLCT) Excited States. Pure Appl Chem. 2013; 85:1257–1305.
3. Zhang Y, Galoppini E, Johansson PG, Meyer GJ. Homoleptic Star-Shaped Ru(II) Complexes. Pure Appl Chem. 2011; 83:861–868.
4. Kärkäs MD, Johnston EV, Verho O, Åkermark B. Artificial Photosynthesis: From Nanosecond Electron Transfer to Catalytic Water Oxidation. Acc Chem Res. 2014; 47:100–111. [PubMed: 23957573]
5. Hammarström L. Accumulative Charge Separation for Solar Fuels Production: Coupling Light-Induced Single Electron Transfer to Mulitelectron Catalysis. Acc Chem Res. 2015; 48:840–850. [PubMed: 25675365]

6. Hartings MR, Kurnikov IV, Dunn AR, Winkler JR, Gray HB, Ratner MA. Electron Tunneling Through Sensitizer Wires Bound to Proteins. Coord Chem Rev. 2010; 254:248–253. [PubMed: 20161508]
7. Anderson BL, Maher AG, Nava M, Lopez N, Cummins CC, Nocera DG. Ultrafast Photoinduced Electron Transfer from Peroxide Dianion. J Phys Chem B. 2015; 119:7422–7429. [PubMed: 25635708]
8. Lo KKW, Li SPY. Utilization of the Photophysical and Photochemical Properties of Phosphorescent Transition Metal Complexes in the Development of Photofunctional Cellular Sensors, Imaging Reagents, and Cytotoxic Agents. RSC Adv. 2014; 4:10560–10585.
9. King A, McClure BA, Jin Y, Rack JJ. Investigating the Effects of Solvent on the Ultrafast Dynamics of a Photoreversible Ruthenium Sulfoxide Complex. J Phys Chem A. 2014; 118:10425–10432. [PubMed: 25137451]
10. Weidmann AG, Komor AC, Barton JK. Targeted Chemotherapy with Metal Complexes. Comments Inorg Chem. 2014; 34:114–123.
11. Knoll JD, Turro C. Control and Utilization of Ruthenium and Rhodium Metal Complex Excited States for Photoactivated Cancer Therapy. Coord Chem Rev. 2015; 282–283:110–126.
12. Joshi T, Gasser G. Towards Tris(diimine)-Ruthenium(II) and Bis(quinoline)-Re(I)$(CO)_3$ Complexes as Photoactivated Anticancer Drug Candidates. Synlett. 2015; 26:275–284.
13. Barragan F, Lopez-Senin P, Salassa L, Betanzos-Lara S, Habtemariam A, Moreno V, Sadler PJ, Marchan V. Photo-controlled DNA Binding of a Receptor-Targeted Organometallic Ruthenium(II) Complex. J Am Chem Soc. 2011; 133:14098–14108. [PubMed: 21797210]
14. Ford PC. Photochemical delivery of nitric oxide. Nitric Oxide. 2013; 34:56–64. [PubMed: 23416089]
15. Howerton BS, Heidary DK, Glazer EC. Strained Ruthenium Complexes Are Potent Light-Activated Anticancer Agents. J Am Chem Soc. 2012; 134:8324–8327. [PubMed: 22553960]
16. Shi G, Monro S, Hennigar R, Colpitts J, Fong J, Kasimova K, Yin H, DeCoste R, Spencer C, Chamberlain L, Mandel A, Lilge L, McFarland SA. Ru(II) Dyads Derived from. α-Oligothiphenes: A New Class of Potent and Versatile, Photosensitizers for PDT Coord. Chem Rev. 2015; 282–283:127–138.
17. (a) Campagna S, Puntoriero F, Nastasi F, Bergamini G, Balzani V. Photochemistry and Photophysics of Coordination Compounds: Ruthenium. Top Curr Chem. 2007; 280:117–214.(b) McCusker JK. Femtosecond Transient Absorption Spectroscopy of Transition Metal Charge-Transfer Complexes. Acc Chem Res. 2003; 36:876–887. [PubMed: 14674779] (c) Juris A, Balzani V, Barigelletti F, Campagna S, Belser P, Von Zelewsky A. Ru(II) Polypyridine Complexes: Photophysics, Photochemistry, Electrochemistry, and Chemiluminescence. Coord Chem Rev. 1988; 84:85–277.(d) Kalyanasundaram K. Photophysics, Photochemistry, and Solar Energy Conversion with Tris(bipyridyl)ruthenium(II) and Its Analogues. Coord Chem Rev. 1982; 46:159–244.
18. Cannizzo A, van Mourik F, Gawelda W, Zgrablic G, Bressler C, Chergui M. Broadband Femtosecond Fluorescence Spectroscopy of $[Ru(bpy)_3]^{2+}$ Angew Chem, Int Ed. 2006; 45:3174–3176.
19. Bhasikuttan AC, Suzuki M, Nakashima S, Okada T. Ultrafast Fluorescence Detection in Tris(2,2′-bipyridine)ruthenium-(II) Complex in Solution: Relaxation Dynamics Involving Higher Excited States. J Am Chem Soc. 2002; 124:8398–8405. [PubMed: 12105921]
20. Anderson NA, Lian T. Ultrafast Electron Injection from Metal Polypyridyl Complexes to Metal-Oxide Nanocrystalline Thin Films. Coord Chem Rev. 2004; 248:1231–1246.
21. (a) Sun Y, Joyce L, Dickson NM, Turro C. Efficient DNA Photocleavage by $[Ru(bpy)_2(dppn)]^{2+}$ with Visible Light. Chem Commun. 2010; 46:2426.(b) Liu Y, Hammitt R, Lutterman DA, Joyce LE, Thummel RP, Turro C. Ru(II) Complexes of New Tridentate Ligands: Unexpected High Yield of Sensitized $^1O_2$. Inorg Chem. 2009; 48:375–385. [PubMed: 19035764]
22. Lincoln R, Kohler L, Monro S, Yin H, Stephenson M, Zong R, Chouai A, Dorsey C, Hennigar R, Thummel RP, McFarland SA. Exploitation of Long-Lived ^{3}IL Excited States for Metal-Organic Photodynamic Therapy: Verification in a Metastatic Melanoma Model. J Am Chem Soc. 2013; 135:17161–17175. [PubMed: 24127659]

23. Ford WE, Rodgers MAJ. Reversible Triplet-Triplet Energy Transfer within a Covalently Linked Molecule. J Phys Chem. 1992; 96:2917–2920.
24. Gu J, Chen J, Schmehl RH. Using Intramolecular Energy Transfer to Transform non-Photoactive, Visible-Light-Absorbing Chromophores into Sensitizers for Photoredox Reactions. J Am Chem Soc. 2010; 132:7338–7346. [PubMed: 20459104]
25. Sun Q, Mosquera-Vazquez S, Daku LML, Guenee L, Goodwin HA, Vauthey E, Hauser A. Experimental Evidence of Ultrafast Quenching of the ^{3}MLCT Luminescence in Ruthenium(II) Tris-bipyridyl Complexes via a ^{3}dd State. J Am Chem Soc. 2013; 135:13660–13663. [PubMed: 24000998] (b) Sun Q, Mosquera-Vazquez S, Suffren Y, Hankache J, Amstutz N, Daku LML, Vauthey E, Hauser A. On the Role of Ligand-Field States for the Photophysical Properties of Ruthenium(II) Polypyridyl Complexes. Coord Chem Rev. 2015; 282–283:87–99.
26. (a) Malouf G, Ford PC. Photochemistry of the Ruthenium-(II) Ammine Complexes, $Ru(NH_3)_5(py\text{-}X)^{2+}$. Variation of Systemic Parameters to Modify Photochemical Reactivities. J Am Chem Soc. 1977; 99:7213–7221.(b) Tfouni E. Photochemical Reactions of Ammineruthenium(II) Complexes. Coord Chem Rev. 2000; 196:281–305.
27. Pinnick DV, Durham B. Temperature Dependence of the Quantum Yields for the Photoanation of $Ru(bpy)_2(L)_2^{2+}$ Complexes. Inorg Chem. 1984; 23:3841–3842.
28. Wacholtz WM, Auerbach RA, Schmehl RH, Ollino M, Cherry WR. Correlation of Ligand Field Excited State Energies with Ligand Field Strength in (Polypyridine)ruthenium(II) Complexes. Inorg Chem. 1985; 24:1758–1760.
29. Durham B, Caspar JV, Nagle JK, Meyer TJ. Photochemistry of $Ru(bpy)_3^{2+}$ J Am Chem Soc. 1982; 104:4803–4810.
30. Sgambellone, MA. PhD Dissertation. The Ohio State University; Columbus, OH: 2013. Photochemistry and Photophysics of Octahedral Ruthenium Complexes.
31. Liu Y, Turner DB, Singh TN, Angeles-Boza AM, Chouai A, Dunbar KR, Turro C. Ultrafast Ligand Exchange: Detection of a Pentacoordinate Ru(II) Intermediate and Product Formation. J Am Chem Soc. 2009; 131:26–27. [PubMed: 19072048]
32. Greenough SE, Roberts GM, Smith NA, Horbury MD, McKinlay RG, Zurek JM, Paterson MJ, Sadler PJ, Stavros VG. Ultrafast Photo-Induced Ligand Solvolysis of cis-$[Ru(bipyridine)_2(nicotinamide)_2]^{2+}$: Experimental and Theoretical Insight into Its Photoactivation Mechanism. Phys Chem Chem Phys. 2014; 16:19141–19155. [PubMed: 25060066]
33. Schrauben JN, Dillman KL, Beck WF, McCusker JK. Vibrational Coherence in the Excited State Dynamics of $Cr(acac)_3$: Probing the Reaction Coordinate for Ultrafast Intersystem Crossing. Chem Sci. 2010; 1:405–410.
34. Garner RN, Joyce LE, Turro C. Effect of Electronic Structure on the Photoinduced Ligand Exchange of Ru(II) Polypyridine Complexes. Inorg Chem. 2011; 50:4384–4391. [PubMed: 21504184]
35. Wachter E, Heidary DK, Howerton BS, Parkin S, Glazer EC. Light-Activated Ruthenium Complexes Photobind DNA and are Cytotoxic in the Photodynamic Therapy Window. Chem Commun. 2012; 48:9649–9451.
36. Von Zelewsky A, Gremaud G. Ruthenium(II) Complexes with Three Different Diimine Ligands. Helv Chim Acta. 1988; 71:1108–1115.
37. Laemmel A-C, Collin J-P, Sauvage J-P. Efficient and Selective Photochemical Labilization of a Given Bidentate Ligand in Mixed Ruthenium(II) Complexes of the $Ru(phen)_2L^{2+}$ and $Ru(bipy)_2L^{2+}$ Family (L = Sterically Hindering Chelate). Eur J Inorg Chem. 1999:383–386.
38. Baranoff E, Collin J, Furusho J, Furusho Y, Laemmel A, Sauvage J. Photochemical or Thermal Chelate Exchange in the Ruthenium Coordination Sphere of Complexes of the $Ru(phen)_2L$ Family (L = Diimine or Dinitrile Ligands). Inorg Chem. 2002; 41:1215–1222. [PubMed: 11874358]
39. Knoll JD, Albani BA, Durr CB, Turro C. Unusually Efficient Pyridine Photodissociaition from Ru(II) Complexes with Sterically Bulky Bidentate Ancillary Ligands. J Phys Chem A. 2014; 118:10603–10610. [PubMed: 25027458]
40. Wachter E, Howerton BS, Hall EC, Parkin S, Glazer EC. A New Type of DNA "Light-Switch": A Dual Photochemical Sensor and Metalating Agent for Duplex and G-Quadruplex DNA. Chem Commun. 2014; 50:311–313.

41. Bonnet S, Collin JP, Sauvage JP, Schofield E. Photo-chemical Expulsion of the Neutral Monodentate Ligand L in Ru(Terpy*)(Diimine)(L)$^{2+}$: A Dramatic Effect of the Steric Properties of the Spectator Diimine Ligand. Inorg Chem. 2004; 43:8346–8354. [PubMed: 15606181]
42. Winkler JR, Netzel TL, Creutz C, Sutin N. Direct Observation of Metal-to-ligand Charge-Transfer (MLCT) Excited States of Pentaammineruthenium(II) Complexes. J Am Chem Soc. 1987; 109:2381–2392.
43. Siemeling U, Vor der Bruggen J, Vorfeld U, Neumann B, Stammler A, Stammler H, Brockhinke A, Plessow R, Zanello P, Laschi F, de Biani FF, Fontani M, Steenken S, Stapper M, Gurzadyan G. Ferrocenyl-Functionalised Terpyridines and Their Transition-Metal Complexes: Syntheses, Structures and Spectroscopic and Electrochemical Properties. Chem - Eur J. 2003; 9:2819–2833. [PubMed: 12866548]
44. Liu Y, Hammitt R, Lutterman DA, Thummel RP, Turro C. Marked Differences in Light-Switch Behavior of Ru(II) Complexes Possessing a Tridentate DNA Intercalating Ligand. Inorg Chem. 2007; 46:6011–6021. [PubMed: 17567125]
45. Sun Y, Liu Y, Turro C. Ultrafast Dynamics of the Low-Lying ^{3}MLCT States of $[Ru(bpy)_2(dppp2)]^{2+}$ J Am Chem Soc. 2010; 132:5594–5595. [PubMed: 20364825]
46. Albani BA, Peña B, Leed NA, de Paula NABG, Pavani C, Baptista MS, Dunbar KR, Turro C. Marked Improvement in Photoinduced Cell Death by a New Tris-heteroleptic Complex with Dual Action: Singlet Oxygen Sensitization and Ligand Dissociation. J Am Chem Soc. 2014; 136:17095–17101. [PubMed: 25393595]
47. Carneiro ZA, de Moraes JCB, Rodrigues FP, de Lima RG, Curti C, da Rocha ZN, Paulo M, Bendhack LM, Tedesco AC, Formiga ALB, da Silva RS. Photocytotoxic activity of a nitrosyl phthalocyanine ruthenium complex – A system capable of producing nitric oxide and singlet oxygen. J Inorg Biochem. 2011; 105:1035–1043. [PubMed: 21726765]
48. Knoll JD, Albani BA, Turro C. Excited State Investigation of a New Ru(II) Complex for Dual Reactivity with Low Energy Light. Chem Commun. 2015; 51:8777–8780.

Biographies

Jessica D. Knoll received her B.S. in chemistry from the University of Dayton in 2008. In 2013, she earned her Ph.D. from Virginia Tech with Prof. Karen Brewer, and she is currently a postdoctoral researcher with Prof. Claudia Turro at The Ohio State University.

Bryan A. Albani received his B.A. in chemistry from The College of Wooster in 2010. He obtained his Ph.D. in 2015 under the supervision of Prof. Claudia Turro at The Ohio State University and is employed as an Advanced Research Scientist at Owens Corning.

Claudia Turro was born in Argentina and received her B.S. and Ph.D. in chemistry at Michigan State University with Profs. Daniel Nocera and George Leroi. Her graduate work on ultrafast proton-coupled electron transfer and excited states of inorganic complexes was followed by research on the interactions of metal complexes with DNA at Columbia University with Prof. Nicholas Turro as a Jane Coffin Childs Memorial Fellow. She began her independent career as a faculty member at The Ohio State University in 1996.

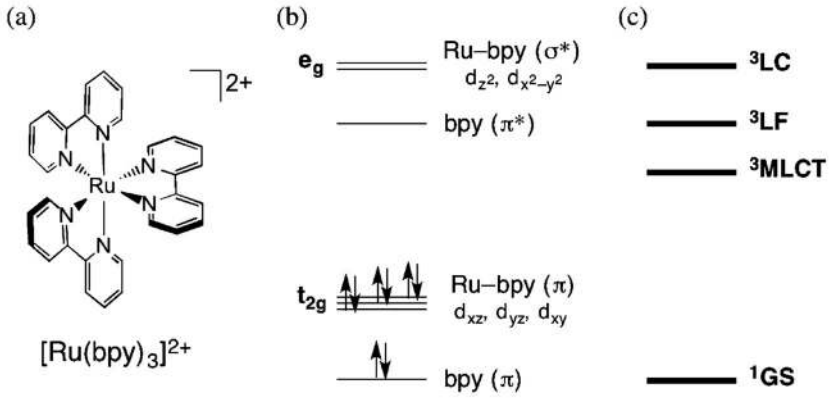

Figure 1.

(a) Molecular structure and simplified (b) MO and (c) state diagrams of $[Ru(bpy)_3]^{2+}$.

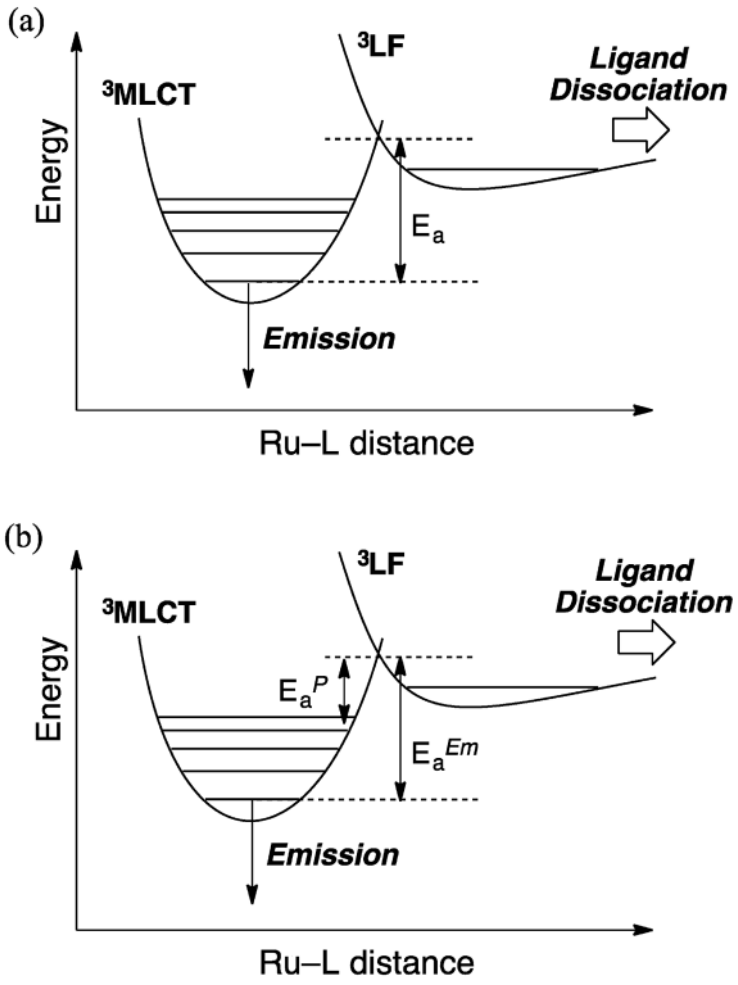

Figure 2.

Schematic representation of the potential energy surfaces showing (a) the activation energy, E_a, for going from ^{3}MLCT$_{v=0}$ to the ^{3}LF state and (b) the proposed sources of E_a^{Em} and E_a^{P}.

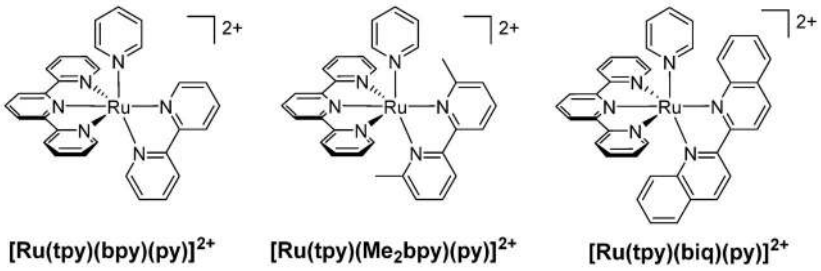

Figure 3.
Structural representations of $[Ru(tpy)(L)(py)]^{2+}$ (NN = bpy, Me_2bpy, biq).

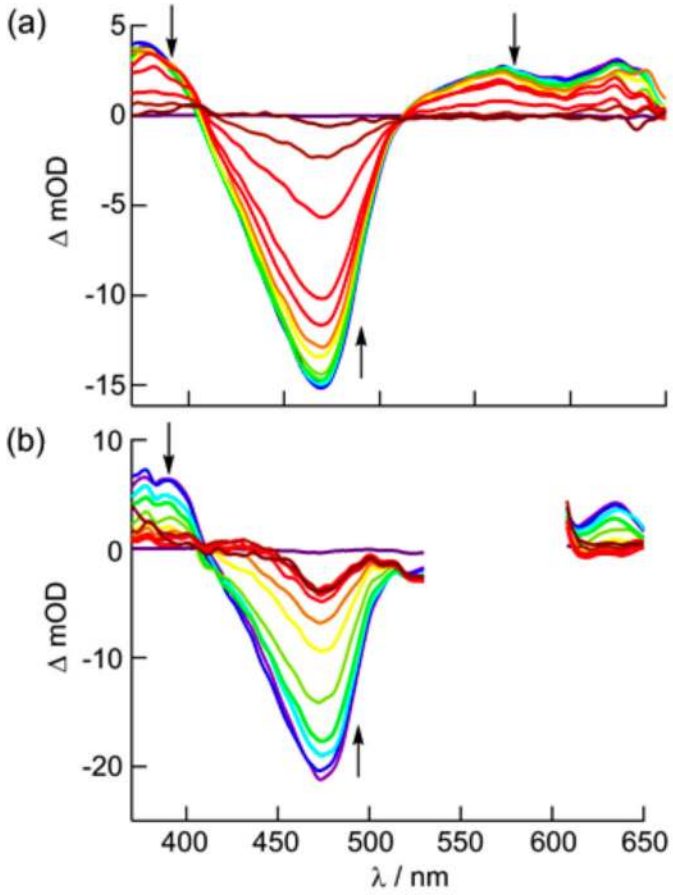

Figure 4.

Transient absorption spectra of (a) $[Ru(tpy)(bpy)(py)]^{2+}$ (λ_{exc} = 350 nm) and (b) $[Ru(tpy)(Me_2bpy)(py)]^{2+}$ (λ_{exc} = 568 nm) in CH_3CN collected 1, 5, 10, 20, 40, 60, 100, 200, 500, 1000, and 2000 ps following the laser pulse (fwhm = 300 fs, baseline collected at −10 ps).

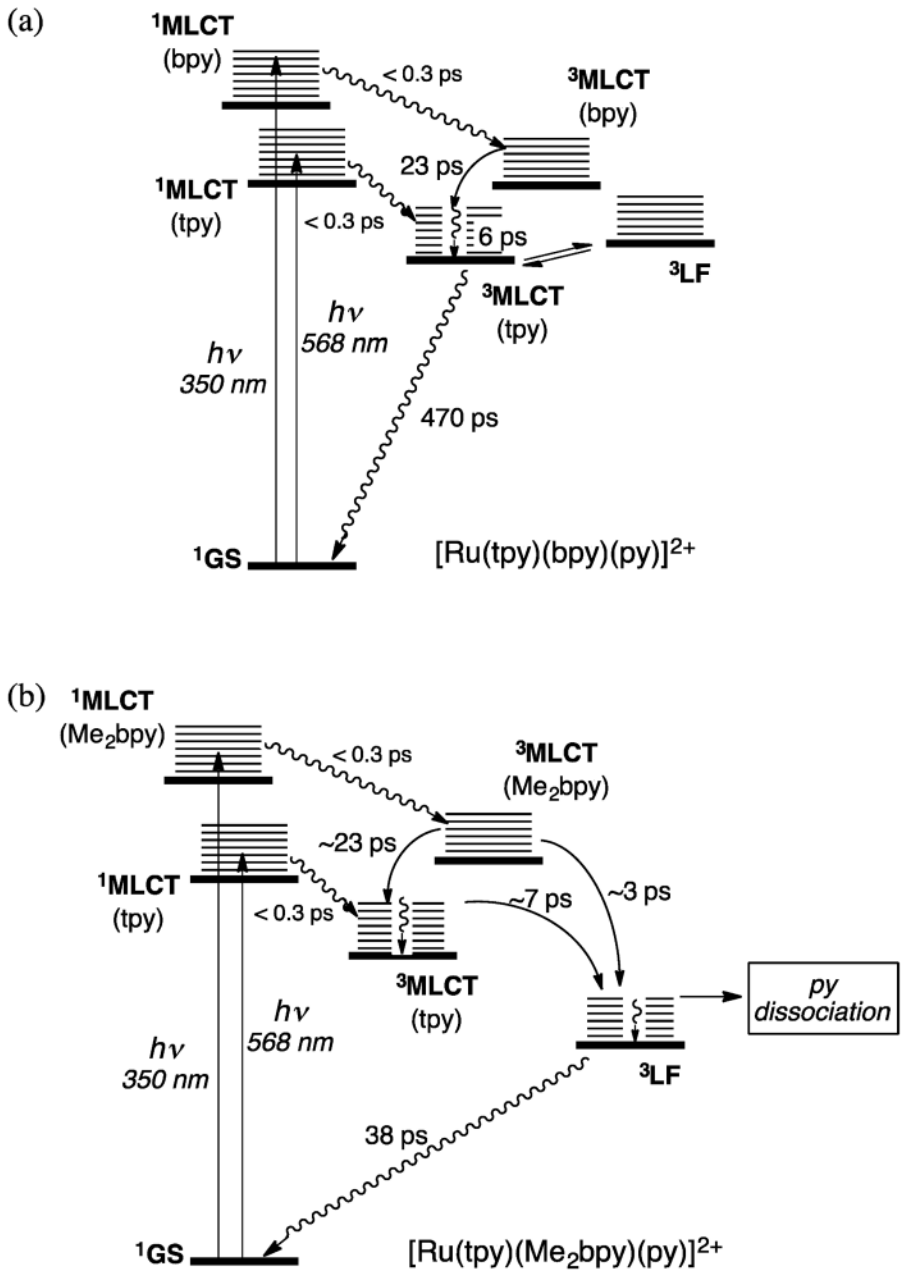

Figure 5.
Jablonski diagrams for (a) $[Ru(tpy)(bpy)(py)]^{2+}$ and (b) $[Ru(tpy)(Me_2bpy)(py)]^{2+}$.

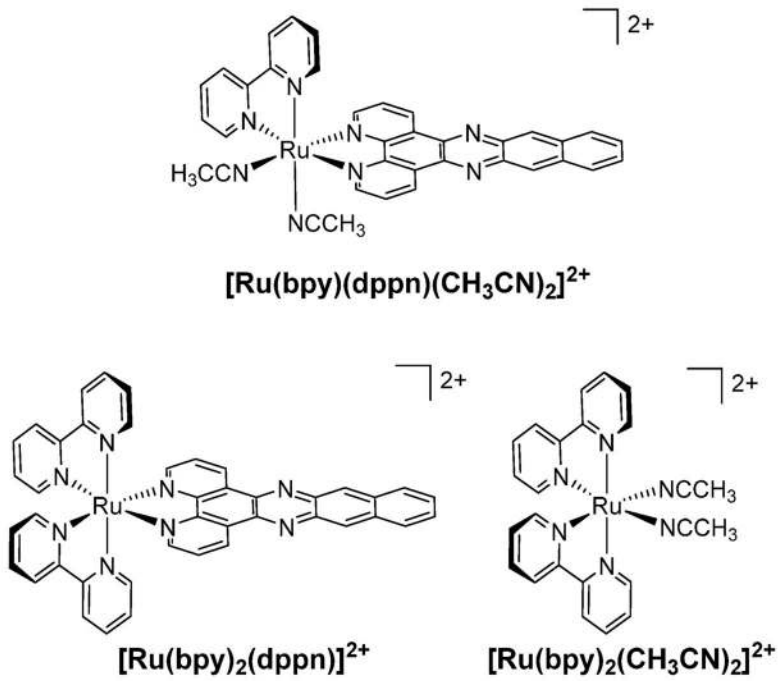

Figure 6.

Structural representations of $[Ru(bpy)(dppn)(CH_3CN)_2]^{2+}$, $[Ru(bpy)_2(dppn)]^{2+}$, and $[Ru(bpy)_2(CH_3CN)_2]^{2+}$.

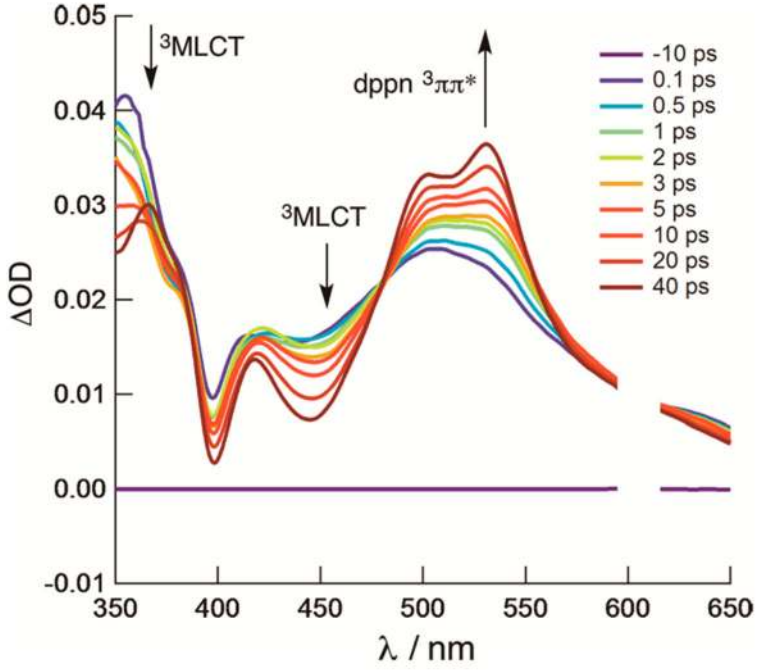

Figure 7.

Transient absorption spectra of $[Ru(bpy)(dppn)\text{-}(CH_3CN)_2]^{2+}$ in CH_3CN (λ_{exc} = 300 nm, fwhm = 300 fs).

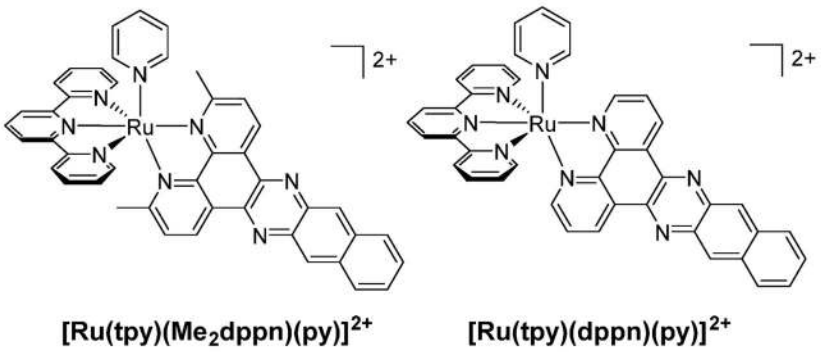

[Ru(tpy)(Me$_2$dppn)(py)]$^{2+}$ [Ru(tpy)(dppn)(py)]$^{2+}$

Figure 8.
Structural representations of [Ru(tpy)(Me$_2$dppn)(py)]$^{2+}$ and [Ru(tpy)(dppn)(py)]$^{2+}$.

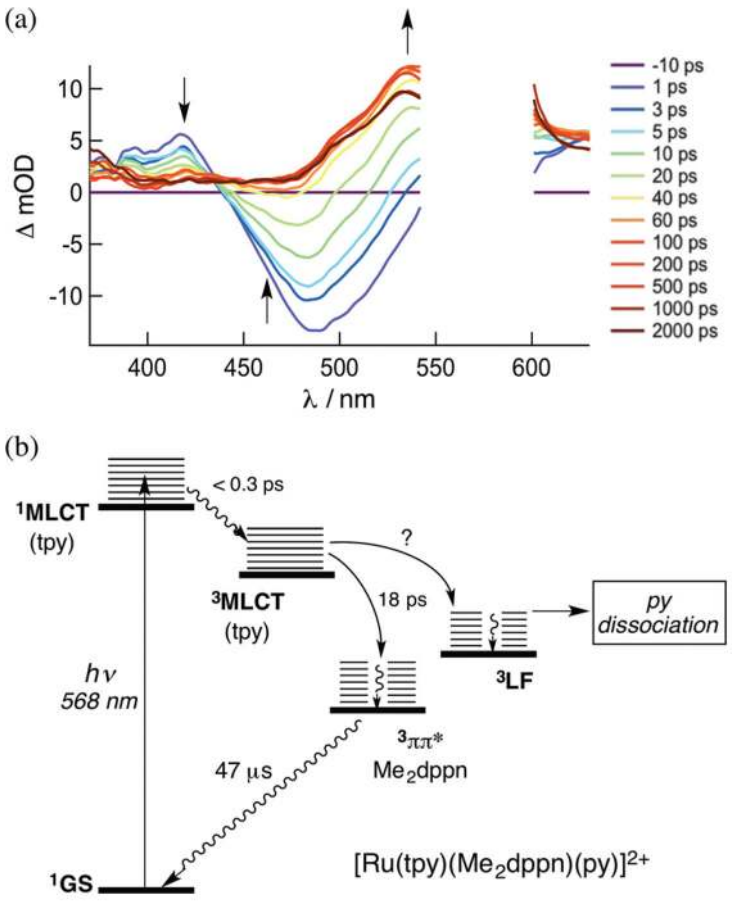

Figure 9.

(a) Ultrafast transient absorption of $[Ru(tpy)(Me_2dppn)\text{-}(py)]^{2+}$ in CH_3CN (λ_{exc} = 568 nm, fwhm = 300 fs) and (b) the corresponding Jablonski diagram.

Table 1

Quantum Yields of Photoinduced Ligand Exchange for $[Ru(bpy)_2(L)_2]^{2+}$ Complexes, Absorption Maxima, and Activation Barriers with the Corresponding Temperature Ranges

L	Φ_{Cl}[a]	λ_{abs}/nm[b]	E_a^{Em}/cm^{-1}[c]	E_a^{P}/cm^{-1}[c]	T/K
CH_3CN	0.31	420	1310 ± 65	515 ± 100	130–170
py	0.17	460	2040 ± 100	940 ± 85	180–230

[a] At 25 °C in CH_2Cl_2 with 20 mM TBACl (λ_{irr} = 400 nm).

[b] In H_2O.

[c] Irradiated at the absorption maximum.

Table 2

Quantum Yields of Ligand Exchange, Φ_{LE}, and $^1O_2$ production, Φ_Δ, for Selected Complexes

complex	Φ_{LE} [a]	Φ_Δ [b]
$[Ru(tpy)(bpy)(py)]^{2+}$	$<10^{-4}$	
$[Ru(tpy)(Me_2bpy)(py)]^{2+}$	0.16(1)	
$[Ru(tpy)(biq)(py)]^{2+}$	0.033(1)	
$[Ru(tpy)(dppn)(py)]^{2+}$	$<10^{-4}$	0.98(6)
$[Ru(tpy)(Me_2dppn)(py)]^{2+}$	0.053(1)	0.69(9)

[a] CH_3CN, λ_{irr} = 500 nm.

[b] MeOH, λ_{irr} = 460 nm.